Hindawi
Journal of Chemistry
Volume 2019, Article ID 3720308, 8 pages
https://doi.org/10.1155/2019/3720308

Research Article

A Reversible Spectrophotometric Method Based on a Coupled Microfluidic Chip for Highly Selective Ammonium Detection

Hao Zhou, Yilin Song, and Zheng Yang

State Key Laboratory of Clean Energy Utilization, Zhejiang University, Hangzhou 310027, China

Correspondence should be addressed to Hao Zhou; zhouhao@cmee.zju.edu.cn

Received 24 September 2019; Revised 5 November 2019; Accepted 14 November 2019; Published 7 December 2019

Academic Editor: Yujiang Song

A coupled chip aiming at economical and highly selective ammonium detection was fabricated. It consisted of a reaction chip, a gas-diffusion chip, and a detection chip. Zinc tetraphenylporphyrin dyed on the cation-exchange resin microbeads was used as the indicating material to avoid excess consumption for its reversibility. PDMS was selected as the material of the gas-diffusion membrane. A portable spectrometer was applied for spectrum analysis. By analysis of spectrum change, the high selectivity was confirmed because no component had interference on detection effect. Good performance was shown for all the tested concentrations (0.2–50 mg·L^{-1}). The stability and reversibility were also judged by the spectrum data obtained from the indicating process and the recovering process. Finally, real samples containing ammonium were tested and the results were compared to those came from a standard method to confirm the accuracy of our method.

1. Introduction

Spectrophotometry is a common optical technique in the microfluidic detection area [1]. It is established on the color change which occurs during the reaction of the selected indicator material and the component to be detected. Then, a spectrometer is applied to measure the spectrum intensity variation for a specific wavelength and thus to obtain the quantity of the required element. Apart from its simplicity, rapidity, and accuracy, spectrophotometry is liable to be involved in the microfluidic chip (MC) aiming at multicomponent detection [2, 3]. Compared to the MC which uses the electrode for detection (another common technique) [4, 5], the MC using the spectrophotometry has a more simplified structure and would not suffer from the electrode degeneration or other electrode-related problems. But spectrophotometry is easy to be interfered with for the reason that the indicator may react with other components, especially those which have similar chemical construction [6]. As a result of low selectivity, the detection sample normally needs to be pretreated (unless the sample is free of interference for sure). When the component to be detected is a kind of volatile gas or can be converted into a volatile element, the gas-diffusion (GD) structure is always preferred for the convincing pretreatment effect [7, 8]. The core unit of a GD structure is a piece of gas-diffusion membrane. The donor solution (usually alkaline) which contains the detection component flows on one side of the GD membrane, and the acceptor solution (acid or neutral) into which the detection component diffuses into flows on the other side. With the development of the microfluidics [9], application of the MC involving the GD structure has attracted much attention because the GD process turns out to be more rapid in the microchannel, which correspondingly intends to perform fast, accurate and integrated detection.

Ammonium (NH_4^+) is one of the numerous kinds of components which can be detected by the MC that consists of the GD and spectrometric structure. Except for various ammonium salts, ammonia (NH_3) which is one of the most common components present in the atmosphere of the earth will also form NH_4^+ when absorbed either by water or acid solution. To eliminate the interference and realize the accurate NH_4^+ detection in a complex environment, NH_4^+ is mostly turned into NH_3 under alkaline condition. The formed NH_3 then diffuses into the acceptor solution through the GD membrane and then followed by the spectrometric

detection [10]. Previous work has utilized polypropylene (PP) [11], polydimethylsiloxane (PDMS) [12], polytetrafluoroethylene (PTFE) [13], and polyvinylidene fluoride (PVDF) [14] as the GD membranes to realize the diffusion and detection of NH_3. Though these membranes have many similarities like hydrophobicity and gas permeability, they vary significantly in many aspects such as mechanical strength and GD efficiency. A key issue in the composition of the GD structure is to find the most suitable MC material (glass, PDMS, cyclic olefin copolymer, or other materials) and the proper bonding technique to seal the GD structure tightly without any leakage [15].

After the diffusion stage, the NH_3 will react with the indicator and present a specific color change, recorded by using the spectrometer. Indophenol blue [16], Nessler [17], bromophenol blue (BTB) [18], and many other reagents [19, 20] have been utilized as the indicator materials.

The typical composition of a GD structure is donor solution-GD membrane-acceptor solution. The donor solution and the acceptor solution are both flowing constantly as a result. Due to the steady donor of NH_3, the constant flow of the donor solution is unavoidable. On the other hand, the acceptor solution which contains the indicator usually has a similar or same flow rate to accept the diffuse NH_3. This means that large amounts of the indicator material are consumed during the process of spectrometric detection. The excess consumption of the indicator material can be indeed attributed to two aspects: first, the indicator material is dissolved in the solution, so the dosage of the acceptor solution determines the consumption amounts of the indicator material. Furthermore, repeatable experiments are always needed to confirm stability and robustness. Second, the reaction of the indicator and NH_3 (NH_4^+) is irreversible. There is no way to turn the indicator back into what it was originally once it reacts with NH_3 (NH_4^+), which means the indicator is nonreusable and can be used only once.

Previous work is mainly focused on the search for a superior indicator material or the optimization of the GD structure. Few researchers pay attention to the irreversible consumption of the indicator, in fact, though it is a significant issue. In allusion to this phenomenon, we combine a GD chip with a kind of reversible indicator, zinc tetraphenylporphyrin (ZnTPP), to conduct NH_4^+ detection. Porphyrins are frequently used as an indicator for the detection of various pollutants in recent years [21–23]. Among the porphyrins, ZnTPP is particularly sensitive to NH_3 and the detection limit can be as low as several ppb. But it suffers from the poor selectivity because the indicating process is based on Lewis acid and bases theory. Acting as Lewis acid, ZnTPP can react with NH_3 as well as many other kinds of Lewis bases like NO [24], $NaHCO_3$, NaOH, and pyridine [25]. So it is challenging to directly detect NH_3 by ZnTPP in a complex condition. In our work, NH_4^+ detection is performed by flow injection analysis (FIA) technique [26] and using a coupled chip (CC) consisting of a reaction chip (RC), a GD chip (GDC), and a detection chip (DC). Our detection remedies the disadvantage of poor selectivity by the GDC so the indicating process is free of interference. The novel immobilization of ZnTPP in the DC and the reversibility of the indicating reaction successfully avoid the constant consumption of the indicating material. The CC which involves a PDMS GD membrane and a portable spectrometer plays the vital analytical roles. The results show splendid performance in quite a wide range with high selectivity. Meanwhile, the spectrum data confirm great stability and enduring reversibility. Finally, real samples that contain various contents of NH_4^+ are tested, and the results are compared to those obtained by a standard method to demonstrate the accuracy of our method.

2. Experimental

2.1. Reagents and Materials. The photoresist (SU-8 2015, MicroChem), single face, polished silicon wafers (4 inches, bought in Hangzhou, China) and PDMS (DC-184, Dow Corning) were used for fabrication of the RC and DC. The GDC was mainly made of glass slides coated with 145 nm chrome and 570 nm photoresist (bought from Shaoguan Chrome Blank Company, China). ZnTPP (5,10,15,20-tetraphenyl-21H,23H-porphine zinc, J&K) dyed on the cation-exchange resin microbeads (Dowex 50WX4 hydrogen form, J&K) was the indicating material. The detailed dying process can be seen in the previous work [25]. The dyed microbeads were washed by alcohol (bought from Sinopharm Chemical Reagent Co., Ltd.) constantly until the percolate became thoroughly transparent. Ammonium chloride (NH_4Cl, Aladdin) was dissolved in various amounts of deionized water to get the corresponding solution. 1 M of sodium hydroxide (NaOH, Sinopharm Chemical Reagent Co., Ltd.) and 0.1 M of ethylenediaminetetraacetic acid (EDTA, Sinopharm Chemical Reagent Co., Ltd.) were mixed to react with NH_4Cl. Deionized water was used as the acceptor solution.

2.2. Fabrication of the CC

2.2.1. Fabrication of the RC. A standard process of photolithography which can be seen in our previous work [27] was applied, and the fabricated RC is shown in Figure 1. The depth and width of the microchannel were both 100 μm. The winding design offered the reactants sufficient time and space to produce NH_3. The total length of the microchannel in which the two reactants reacted was about 420 mm according to our calculation.

2.2.2. Fabrication of the GDC. The GDC was made of two glass chips with a piece of GD membrane in the middle. The fabrication process of glass chips can be read in other works [28]. The GD membrane was made of PDMS. Though the PDMS membrane was not the best in mechanical strength compared to PVDF or PTFE, it could be bonded tightly without any leakage to glass chips after plasma treatment. We made a piece of 10 μm membrane according to the method in an earlier paper [12]. The thickness considered two aspects: an excessive thick membrane would decrease the GD efficiency and an unduly thin membrane would reduce the mechanical strength as well as the service life. The

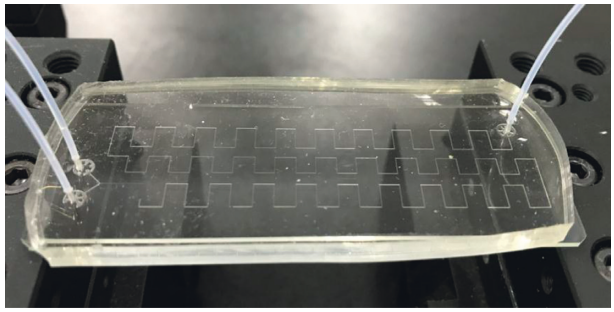

Figure 1: The RC.

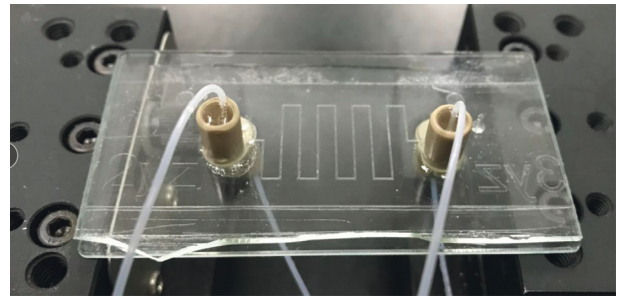

Figure 2: The GDC.

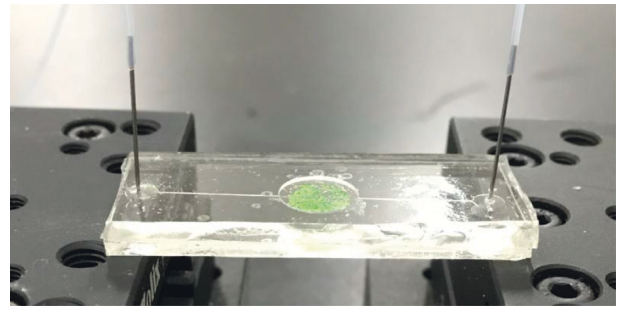

Figure 3: The DC.

microchannels in top glass chip and bottom glass chip were both 50 μm in depth and 300 μm in width. The high width-to-depth ratio provided a large contact area between the solution and the membrane and helped increase the GD efficiency. But the microchannel could not be too wide in case that the GD membrane would wrinkle. The GDC is shown in Figure 2. Though the GD microchannels of the top chip and the bottom chip matched perfectly, the inlets and outlets were staggered to avoid damage of the GD membrane due to the larger pressure. An assistant circular mark was etched at the same position of each chip for better alignment. The total length of the GD channel was about 148 mm.

2.2.3. Fabrication of the DC. A 4-layer chip which could be seen in Figure 3 was fabricated for NH_3 detection. The mixture made of DPMS and curing agent at a ratio of 10 : 1 was coated on the glass slide at the speed of 4000 r/min to form an immobilization layer with the thickness of 24 μm. Then, a glass slide (0.5 mm thick) with a penetrating hole (diameter: 10 mm) was placed on the immobilization layer. 10 mg of ZnTPP-dyed cation-exchange resin microbeads was uniformly placed on the layer through the penetrating hole. The stack was heated at 80°C for 5 h under vacuum condition so that the immobilization layer became solidified. The top PDMS chip was also fabricated by standard photolithography. The left channel and right channel have an abruption of 8 mm. Finally, the top PDMS chip was bonded with the 3-layer stack by plasma treatment. Make sure that both the left channel and the right channel were connected to the penetrating hole.

2.2.4. Fabrication of the CC. The schematic of the CC, as well as the detailed structure of the RC, GDC, and DC, can be seen in Figure 4. The arrows show the flowing direction. R1–R7 represented various reagents. R1 represented the NH_4Cl solution which was pumped into the RC by using syringe pump 1 (Elite Pump 11, Harvard). R2 represented the solution of NaOH + EDTA which was pumped into the RC by using syringe pump 2 (Elite Pump 11, Harvard). R1 and R2 then reacted in the RC and formed the donor solution (R3) which contained NH_3. R3 was turned into R4 (the waste) after NH_3 diffused from the donor solution into the acceptor solution (R5). R5 was pumped into the GDC by using syringe pump 3 (Elite Pump 11, Harvard). R6 represented the formed NH_3 solution and flowed into the DC. R7 was the waste after the indicating and detection process.

2.3. Integrated System. Figure 5 demonstrates the schematic of the integrated system. A white LED light with a collimator tightly attached was used to produce a narrow beam of parallel light. The beam was focused into the fiber by using a lens (LA1131-A-ML, $f = 50.0$ mm, Thorlabs) after passing through the penetrating hole and the ZnTPP-dyed microbeads. The spectrum was then analyzed by using the portable spectrometer (USB 650, Ocean Optics) and recorded using by the PC.

3. Results and Discussion

3.1. Highly Selective Detection Performance. The injection rates of syringe pump 1 and syringe pump 2 were both 1 μL·min^{-1}, while that of syringe pump 3 was 2 μL·min^{-1}. With the exposure time being 8 ms, the spectrometer worked in the continuous model and recorded the spectrum data at 10 s each. The recording wavelength ranged from 200 nm to 800 nm. The dark spectrum was recorded and subtracted first to avoid interference. A reference spectrum was recorded by using deionized water as R1, R2, and R3, and the recording time was 10 min. Then, NaOH + EDTA was used as R2 while R1 and R3 used deionized water for 30 min. The spectrum of this period was recorded as the contrast spectrum. Finally, the NH_4^+ solution of various concentrations (the order of test was from high concentration to low concentration) was used as R1 for 30 min and the spectrum was recorded as the detection spectrum. This process was followed by another 30 min of recording with R1, and R2 changed into deionized water again. Thus, a cycle

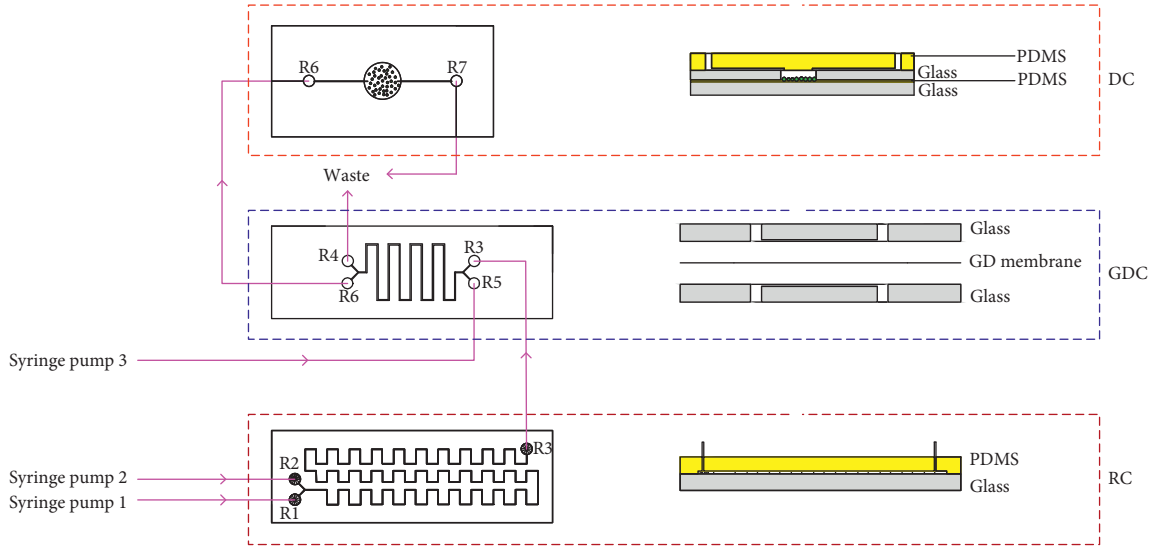

Figure 4: Schematic of the CC and the detailed structure of the RC, GDC, and DC.

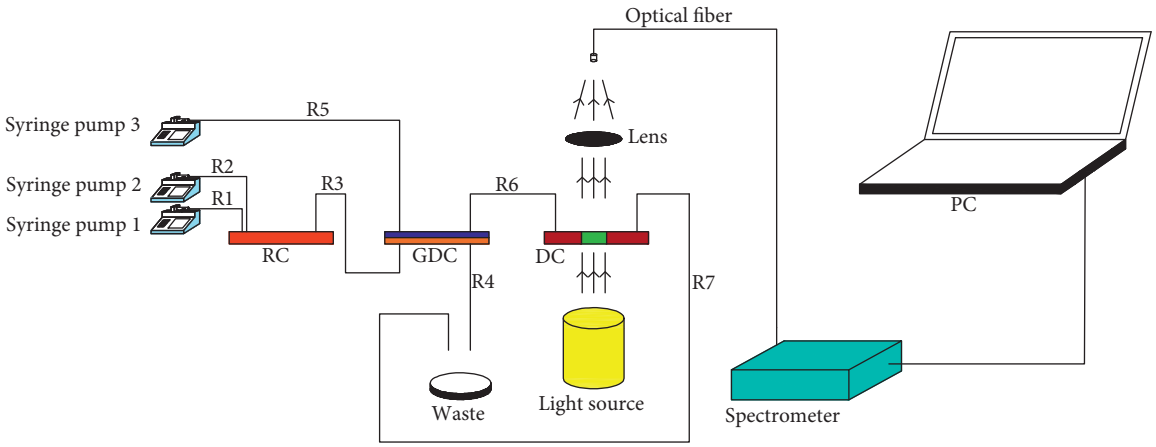

Figure 5: Schematic of the integrated system.

was formed for the detection process. 10 cycles of tests were conducted for each concentration. All spectrums were normalized to their maximal intensity, and the normalized reference spectrum, contrast spectrum, and detection spectrum were expressed as S_r, S_c, and S_d.

Due to the reaction with NH_3, ZnTPP would turn from green to purple in the indicating stage. So compared to the S_r, the light intensity of the S_d would increase in the purple range (430–470 nm) and decrease in the green range (500–550 nm). As far as we know, the decrease in the green color was not as obvious as the increase in the purple color. The spectrum intensity change was particularly remarkable at the wavelength of 450 nm. Therefore, we used the spectrum intensity at 450 nm for all the spectrum analysis and introduced two parameters:

$$\begin{aligned} \Delta S_c &= S_c - S_r, \\ \Delta S_d &= S_d - S_r, \end{aligned} \tag{1}$$

where ΔS_c represented the contrast spectrum change and ΔS_d represented the detection spectrum change.

Figure 6 showed the detection results for various NH_4^+ concentrations. For a certain concentration, ΔS_d is the average of 10 results obtained after the color change (from green to purple) had become steady. In the alkaline condition of our experiments, no acid interference existed obviously. In fact, the most possible interference was the excess NaOH which was used for NH_3 production. We could know from previous work [25] that NH_3 solution with a concentration of c% and NaOH solution with a concentration of 20c% had similar effects on ZnTPP. In our experiments, the concentration of NaOH was much higher than that of the formed NH_3 solution for a thorough conversion of NH_4^+. During the 30 min contrast test, the average ΔS_c was merely 0.0006. It meant that the spectrum change was negligible because it is much smaller when compared to ΔS_d of 0.2 mg·L^{-1} (about 0.0082). It indicates that ZnTPP did not react with the hydroxide anion in the solution when only the NaOH solution was injected. Owing to the existence of GDC, OH^- would not interfere with the detection. Meanwhile, we could see the good detection performance for NH_4^+ from ΔS_d. It represents the result of

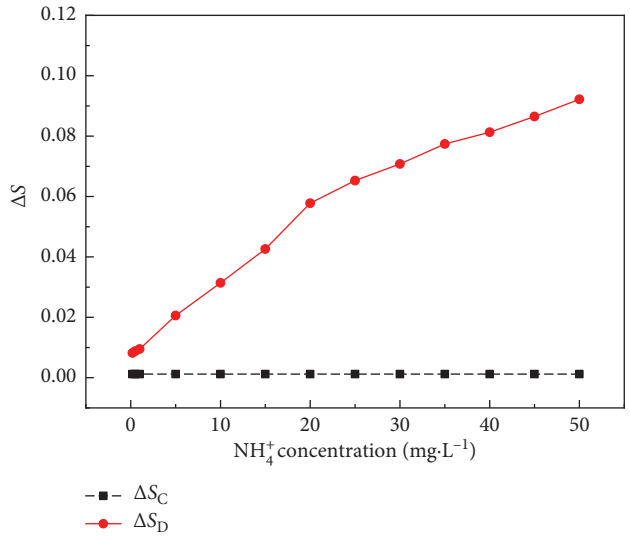

Figure 6: The detection results for various NH_4^+ concentrations.

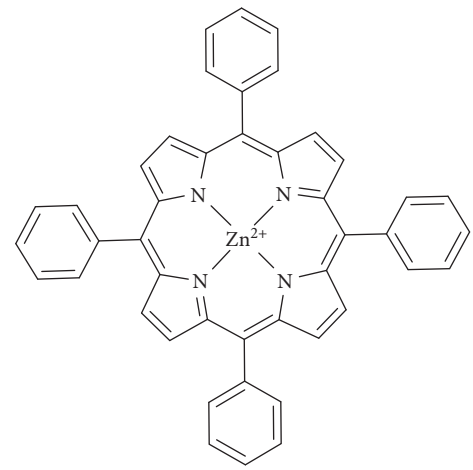

Figure 7: The structure of ZnTPP.

selective ammonia detection under complex alkaline conditions.

For a very wide range (0.2–50 mg·L^{-1}), ΔS_d had a relatively high value. However, the detection of a low concentration of NH_4^+ is more linear than that of high concentration. Because the amount of NH_3 is small at a low concentration, where NH_3 can sufficiently contact ZnTPP dyed on the microbeads. This is why the measurement is more sensitive. At high concentrations, due to the limited surface area of the microbeads, a small amount of ammonia may not contact ZnTPP and pass through the indicator area. It results in a lower correlation of ammonia detection. However, from the overall trend, ΔS_d forms a good linear relationship with NH_4^+ concentration. According to our test, the detection limit was about 0.1 mg·L^{-1}. Furthermore, ΔS_d varied to a large extent as the NH_4^+ concentration increased. When NH_4^+ concentration was 1 mg·L^{-1}, ΔS_d was merely 0.0095. But the value increased to 0.0206 as the NH_4^+ concentration rose to 5 mg·L^{-1}. It should be noted that even for low NH_4^+ concentrations (<1 mg·L^{-1}), the detection showed splendid and stable results. In our experiments, ΔS_d values for 0.2 mg·L^{-1}, 0.5 mg·L^{-1}, and 1 mg·L^{-1} were 0.0082, 0.0088, and 0.0095. The results were all average of 10 tests.

3.2. Reversible Indicating Process. ZnTPP is metal ion-containing organic dyes that respond to analytes capable of the Lewis acid and bases interactions. Its structure is shown in Figure 7. The reaction of ZnTPP with NH_3 can be explained by the Lewis acid and bases theory. On the one hand, the ZnTPP molecule contains an empty orbital. Therefore, it is an acid that can bind to some molecules containing the lone pair of electrons. On the other hand, NH_3 is such a molecule that can also be used as a Lewis base.

ZnTPP was selected as the indicating material because the indicating reaction was reversible, compared to the other materials like BTB. When ZnTPP dyed on the microbeads contacted NH_3, it would accept the lone pair of electrons of the NH_3 molecule and turn from green to purple. This process is the indicator process. However, once there was no NH_3 molecule in the surrounding environment, the product that had been generated would be decomposed, and NH_3 would escape from ZnTPP and enter deionized water, which caused ZnTPP to turn from back to green. This process is the recovery process. As shown in Figure 8, each cycle was divided into indicating process (from green to purple) and recovering process (from purple to green). Figure 9 shows the ΔS_d of 10 cycles for 20 mg·L^{-1}.

According to the results, for NH_4^+ concentration of 20 mg·L^{-1}, the average time of the indicating process was about 7.2 min. For the entire tested concentrations, the average indicating time increased slightly with the increased NH_4^+ concentration. The average indicating time for 0.2 mg·L^{-1} was 5.8 min while that increased to 9.1 min for 50 mg·L^{-1}. A similar trend was observed in the recovering process. The average recovering time for 0.2 mg·L^{-1} was about 11 min, but that rose to 13.6 min for 50 mg·L^{-1}. For a certain concentration, the recovering time was almost twice as long as the indicating time. We could simultaneously see that the results were fairly stable since the 10 cycles exhibited scarcely any difference. This proved the stability of the detection.

Though ΔS_d of the indicating process varied with NH_4^+ concentration, ΔS_d of the recovering process remained unchanged regardless of NH_4^+ concentration. In other words, ΔS_d of the recovering process could be applied to measure the reversibility.

We extracted the ΔS_d of the indicating process and the recovering process for the 10 cycles under each NH_4^+ concentration. The results were arranged in the experimental order (from high concentration to low concentration), and they are shown in Figure 10. It was obvious that ΔS_d of the recovering process remained at an extremely low level all the time with an average of less than 0.0001. It is confirmed that though ΔS_d of the indicating process varied, ΔS_d of the recovering process remained because of the reversibility. In other words, ZnTPP went back into what it was for the reference spectrum regardless of NH_4^+ concentration.

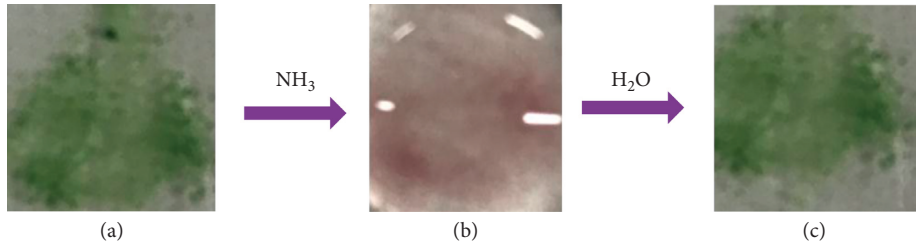

Figure 8: Changes in ZnTPP in each cycle: (a) original state, (b) after reaction with NH_3, and (c) after recovery in pure water environment.

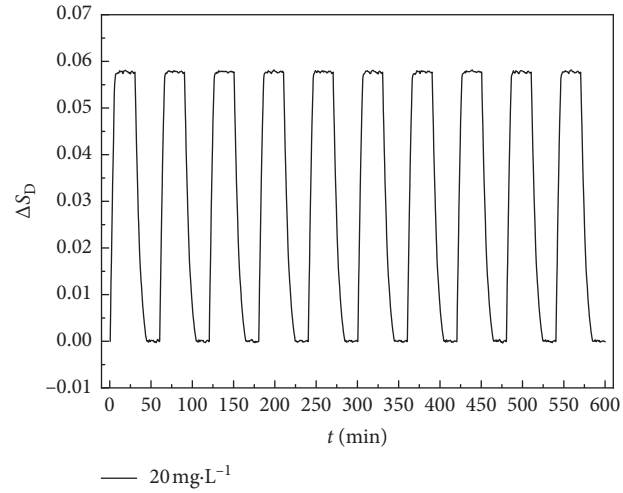

Figure 9: ΔS_d of 10 cycles for 20 mg·L^{-1}.

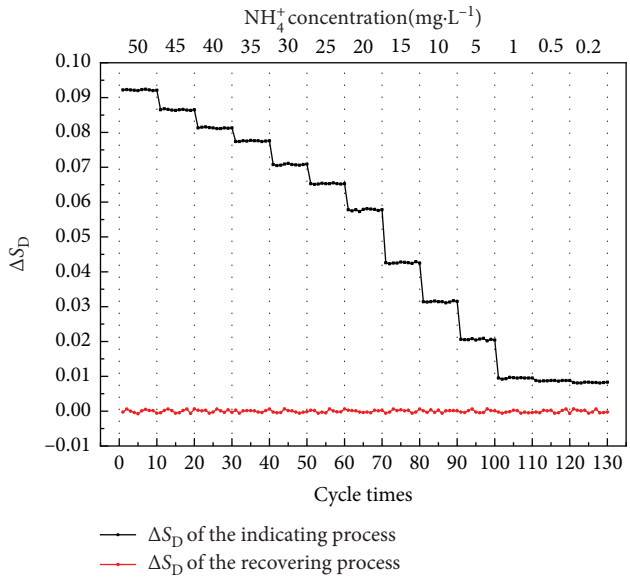

Figure 10: ΔS_d of the indicating process and the recovering process for each cycle.

Totally, 130 cycles of tests were conducted, which demonstrated that the property of ZnTPP had no variation compared to the original state after 130 cycles. On the one hand, the stability and reversibility of ZnTPP were verified. On the other hand, it was illustrated that the remaining parts of the CC worked in suitable condition without any degeneration, such as the PDMS GD membrane. Furthermore, the indicating material we used was the ZnTPP dyed on the microbeads which were immobilized in the DC during the whole experiment. R3 used deionized water all the time instead of various kinds of indicating solutions containing large amounts of the indicating material. So this was obviously an economical method for the reason that it could save large amounts of indicating material during the experiments.

In fact, the economy of the CC was incarnated by another characteristic. Although the GD membrane did not degenerate during our tests, it was well known to all that the membrane was a flimsy part due to its poor mechanical strength. Similarly, the reversibility of ZnTPP was not permanent and it would recede sooner or later. The separating design of our CC allowed us to substitute the broken chip only instead of the entire CC. If the GDC degenerated, for example, it could be replaced by a new GDC without any influence on the RC and DC. The intended replacement of a specific chip helped prolong the service of the CC and bring economic improvement.

3.3. Real Sample Analysis. Ammonium salt is one of the most common detrimental matter in the boilers of power plants and other coal-fired industrial equipment. It can deposit on the surface of the heat exchangers or the catalyst of the denitrification system, causing worse heat exchange or blocking [29, 30]. So the detection of ammonium salt has great industrial significance.

The tested samples were ash deposition obtained from the surface of an ash deposition probe in a drop tube furnace aiming to study the deposition of ammonium salt. The content of ammonium salt varied with the surface temperature of the ash deposition probe. X-ray fluorescence (XRF) results were first analyzed to estimate the approximate content. According to the calculation, the content of ammonium of the four samples ranged from 2% to 35%. 1 g of ash deposition for each sample was dissolved in deionized water, and the obtained solution of 100 mg·L^{-1} was filtered to remove insoluble precipitate, followed by 5 h of static treatment. Then, each sample would be tested. The contrast results came from a standard Berthelot method [14]. For both the two methods, tests were conducted 4 times for each of the 4 samples. The obtained results ($n = 4$, 95% confidence) are shown in Table 1.

As can be seen from Table 1, the results of the two methods were very close for all the 4 samples. The maximal

Table 1: Detection concentrations (mg L^{-1}) for the 4 samples by the two methods.

Sample	1	2	3	4
CC method	2.7 ± 0.3	18.7 ± 0.4	23.2 ± 0.2	29.8 ± 0.1
Berthelot method	2.9 ± 0.2	18.4 ± 0.2	22.6 ± 0.3	30.3 ± 0.2
Error	7%	2%	3%	2%

absolute deviation was 0.6 mg·L^{-1}, and the maximal relative standard deviation was 7%. Considering the fact that the Berthelot method was a relatively mature and accurate technique, the accuracy of our detection was confirmed.

4. Conclusions

In our research, with a CC and a portable spectrometer, we realize NH_4^+ detection by analysis of the spectrum change at the wavelength of 450 nm. The CC consists of an RC, a GDC, and a DC. The RC is used to convert NH_4^+ into NH_3. The GDC which involves a 10 μm PDMS membrane is applied for NH_3 diffusion. The DC is used for NH_3 detection based on the reversible reaction between ZnTPP and NH_3. The CC settles the issues of poor selectivity encountered by ZnTPP when applied in a complex environment. Furthermore, compared to other spectrophotometric methods, the ZnTPP dyed on the microbeads immobilized in the DC realizes high detection without indicating material consumption anymore. By analysis of the spectrum data, we first demonstrated the high selectivity because even the strongest interference of NaOH has no effect on the detection. The detection exhibits good performance in a wide range (0.2–50 mg·L^{-1}) as well as a large extent of variation corresponding with NH_4^+ concentration. Then, through the 130 cycles of tests (10 cycles for each concentration), we confirm the stability and reversibility of the detection. The entire CC can also be proved to be in good condition. Large amounts of indicating material can be saved by our method. Besides, the separating design of our CC allows replacement of the specific broken chip instead of the entire CC. The two points improve the economic property of the proposed method. Finally, we conduct real sample experiments using the ash deposition obtained from an ash deposition probe in a drop tube furnace. By comparison between the results from our method and those from a standard Berthelot method, we obtain a maximal relative standard deviation of 7% and confirm the accuracy of our detection.

Data Availability

The data used to support the findings of this study are available from the corresponding author upon request.

Conflicts of Interest

The authors declare that there are no conflicts of interest regarding the publication of this paper.

Acknowledgments

This work was supported by the National Science Fund for Distinguished Young Scholars (no. 51825605).

References

[1] A. Daridon, M. Sequeira, G. Pennarun-Thomas et al., "Chemical sensing using an integrated microfluidic system based on the Berthelot reaction," *Sensors and Actuators B: Chemical*, vol. 76, no. 1–3, pp. 235–243, 2001.

[2] Y. Zilberman and S. R. Sonkusale, "Microfluidic optoelectronic sensor for salivary diagnostics of stomach cancer," *Biosensors and Bioelectronics*, vol. 67, pp. 976–983, 2015.

[3] H. Hwang, Y. Kim, J. Cho, J.-Y. Lee, M.-S. Choi, and Y.-K. Cho, "Lab-on-a-disc for simultaneous determination of nutrients in water," *Analytical Chemistry*, vol. 85, no. 5, pp. 2954–2960, 2013.

[4] T.-Y. Chiang and C.-H. Lin, "A microfluidic chip for ammonium sensing incorporating ion-selective membranes formed by surface tension forces," *RSC Advances*, vol. 4, no. 1, pp. 379–385, 2014.

[5] A. Calvo-López, O. Ymbern, M. Puyol, J. M. Casalta, and J. Alonso-Chamarro, "Potentiometric analytical microsystem based on the integration of a gas-diffusion step for on-line ammonium determination in water recycling processes in manned space missions," *Analytica Chimica Acta*, vol. 874, pp. 26–32, 2015.

[6] P. L. Searle, "The berthelot or indophenol reaction and its use in the analytical chemistry of nitrogen. A review," *The Analyst*, vol. 109, no. 5, pp. 549–568, 1984.

[7] S.-I. Ohira and K. Toda, "Micro gas analysis system for measurement of atmospheric hydrogen sulfide and sulfur dioxide," *Lab on a Chip*, vol. 5, no. 12, pp. 1374–1379, 2005.

[8] M. T. Oms, A. Cerdà, A. Cladera, V. Cerdà, and R. Forteza, "Gas diffusion techniques coupled sequential injection analysis for selective determination of ammonium," *Analytica Chimica Acta*, vol. 318, no. 3, pp. 251–260, 1996.

[9] A. Manz, N. Graber, and H. M. Widmer, "Miniaturized total chemical analysis systems: a novel concept for chemical sensing," *Sensors and Actuators B: Chemical*, vol. 1, no. 1–6, pp. 244–248, 1990.

[10] R. A. Segundo, R. B. R. Mesquita, M. T. S. O. B. Ferreira, C. F. C. P. Teixeira, A. A. Bordalo, and A. O. S. S. Rangel, "Development of a sequential injection gas diffusion system for the determination of ammonium in transitional and coastal waters," *Analytical Methods*, vol. 3, no. 9, pp. 2049–2055, 2011.

[11] B. H. Timmer, M. van Delft, W. W. Koelmans, W. Olthuis, and A. van den Berg, "Selective low concentration ammonia sensing in a microfluidic lab-on-a-chip," *IEEE Sensors Journal*, vol. 6, no. 3, pp. 829–835, 2006.

[12] K. Toda, S.-I. Ohira, and M. Ikeda, "Micro-gas analysis system μGAS comprising a microchannel scrubber and a microfluorescence detector for measurement of hydrogen sulfide," *Analytica Chimica Acta*, vol. 511, no. 1, pp. 3–10, 2004.

[13] Z. Zhu, J. J. Lu, M. I. G. S. Almeida, Q. Pu, S. D. Kolev, and S. Liu, "A microfabricated electroosmotic pump coupled to a gas-diffusion microchip for flow injection analysis of ammonia," *Microchimica Acta*, vol. 182, no. 5-6, pp. 1063–1070, 2015.

[14] S. M. Oliveira, T. I. M. S. Lopes, I. V. Tóth, and A. O. S. S. Rangel, "A multi-commuted flow injection system with a multi-channel propulsion unit placed before detection: spectrophotometric determination of ammonium," *Analytica Chimica Acta*, vol. 600, no. 1-2, pp. 29–34, 2007.

[15] H. Becker and L. E. Locascio, "Polymer microfluidic devices," *Talanta*, vol. 56, no. 2, pp. 267–287, 2002.

[16] M. Berthelot, *Répertoire Chimie Pure Appliquée 1*, Société Chimique de Paris, Paris, France, 1859.
[17] L. Zhou and C. E. Boyd, "Comparison of Nessler, phenate, salicylate and ion selective electrode procedures for determination of total ammonia nitrogen in aquaculture," *Aquaculture*, vol. 450, pp. 187–193, 2016.
[18] J. Courbat, D. Briand, J. Damon-Lacoste, J. Wöllenstein, and N. F. de Rooij, "Evaluation of pH indicator-based colorimetric films for ammonia detection using optical waveguides," *Sensors and Actuators B: Chemical*, vol. 143, no. 1, pp. 62–70, 2009.
[19] C. Preininger, G. J. Mohr, I. Klimant, and O. S. Wolfbeis, "Ammonia fluorosensors based on reversible lactonization of polymer-entrapped rhodamine dyes, and the effects of plasticizers," *Analytica Chimica Acta*, vol. 334, no. 1-2, pp. 113–123, 1996.
[20] H. S. Mader and O. S. Wolfbeis, "Optical ammonia sensor based on upconverting luminescent nanoparticles," *Analytical Chemistry*, vol. 82, no. 12, pp. 5002–5004, 2010.
[21] R. Paolesse, S. Nardis, D. Monti, M. Stefanelli, and C. Di Natale, "Porphyrinoids for chemical sensor applications," *Chemical Reviews*, vol. 117, no. 4, pp. 2517–2583, 2017.
[22] X.-R. Li, B. Wang, J.-J. Xu, and H.-Y. Chen, "Noncovalent assembly of picket-fence porphyrin on carbon nanotubes as effective peroxidase-like catalysts for detection of hydrogen peroxide in beverages," *Electroanalysis*, vol. 23, no. 12, pp. 2955–2963, 2011.
[23] X. Liu, X. Liu, M. Tao, and W. Zhang, "A highly selective and sensitive recyclable colorimetric Hg^{2+} sensor based on the porphyrin-functionalized polyacrylonitrile fiber," *Journal of Materials Chemistry A*, vol. 3, no. 25, pp. 13254–13262, 2015.
[24] C. Peter, K. Schmitt, M. Apitz, and J. Woellenstein, "Metalloporphyrin zinc as gas sensitive material for colorimetric gas sensors on planar optical waveguides," *Microsystem Technologies*, vol. 18, no. 7-8, pp. 925–930, 2012.
[25] Y. Zilberman, Y. Chen, and S. R. Sonkusale, "Dissolved ammonia sensing in complex mixtures using metalloporphyrin-based optoelectronic sensor and spectroscopic detection," *Sensors and Actuators B: Chemical*, vol. 202, pp. 976–983, 2014.
[26] J. Ṙužička and E. H. Hansen, "Flow injection analyses: part I. A new concept of fast continuous flow analysis," *Analytica Chimica Ada*, vol. 78, pp. 145–157, 1975.
[27] H. Zhou, Z. Yang, Z. Yao, and K. Cen, "Application of digital holographic microscopy and microfluidic chips to the measurement of particle size distribution of fly ash after a wet electrostatic precipitator," *Flow Measurement and Instrumentation*, vol. 60, pp. 24–29, 2018.
[28] Y. Song, Y. Shi, X. Li et al., "Afi-chip: an equipment-free, low-cost, and universal binding ligand affinity evaluation platform," *Analytical Chemistry*, vol. 88, no. 16, pp. 8294–8301, 2016.
[29] Y.-J. Shi, H. Shu, Y.-H. Zhang, H.-M. Fan, Y.-P. Zhang, and L.-J. Yang, "Formation and decomposition of NH_4HSO_4 during selective catalytic reduction of NO with NH_3 over V_2O_5-WO_3/TiO_2 catalysts," *Fuel Processing Technology*, vol. 150, pp. 141–147, 2016.
[30] L. Muzio, S. Bogseth, R. Himes, Y.-C. Chien, and D. Dunn-Rankin, "Ammonium bisulfate formation and reduced load SCR operation," *Fuel*, vol. 206, pp. 180–189, 2017.